JOURNAL OF GUIDANCE, CONTROL, AND DYNAMICS
Vol. 25, No. 5, September–October 2002

# Analytical Modeling of Sensor Quantization in Strapdown Inertial Navigation Error Equations

Paul G. Savage
*Strapdown Associates, Inc., Maple Plain, Minnesota 55359*

**Although generally not considered a major contributor to system inaccuracy, inertial sensor quantization error, if not properly modeled, can lead to erroneously large estimates of its impact on inertial navigation system performance. Analytical methods are described for modeling inertial sensor quantization in strapdown inertial system error parameter propagation and measurement equations. Error propagation equations are derived in classical differential error state dynamic and discrete difference format. It is shown how the attitude, velocity, and sensor error parameters in these equations must be modified to enable proper sensor quantization error modeling as white noise and to account for differences in attitude, velocity, and position update frequencies. The discrete difference error equation form is used to develop values for attitude/velocity measurement noise covariances and for spectral densities of white quantization noise terms in the differential error propagation equations. A general discussion is included of how quantization white noise spectral densities should be computed for the differential error propagation equations for compatibility with two-speed attitude, velocity, and position updating algorithms. Validity limits for white noise modeling approximations and methods for reducing quantization noise are discussed. Numerical examples are provided.**

## Nomenclature

| | | |
|---|---|---|
| $A$ | = | error state dynamic matrix |
| $\boldsymbol{a}_{\text{sf}}^{B}$, $\boldsymbol{a}_{\text{sf}}^{I}$ | = | sensor assembly specific force acceleration vector in $B$ and $I$ frame coordinates (i.e., total acceleration minus gravity, the acceleration sensed by accelerometers in the B frame) |
| $B$ | = | body coordinate frame aligned with strapdown sensor assembly axes at a general time |
| $B_{(\,)}$ | = | frame $B$ orientation (relative to the $I$ frame) at computer cycle time ( ) |
| $C_{(\,)}^{[\,]}$ | = | direction cosine matrix that transforms vectors from coordinate frame ( ) to coordinate frame [ ] |
| $\mathcal{E}(\,)$ | = | expected value operator |
| $f_l$, $f_m$, $f_n$ | = | frequencies for the $l$, $m$, and $n$ attitude, velocity, and position computer update cycles |
| $G_P$ | = | process noise dynamic coupling matrix |
| $\boldsymbol{g}^I$ | = | Earth's mass attraction gravity vector projected on $I$ frame axes |
| I | = | identity matrix |
| $I$ | = | inertially nonrotating coordinate frame |
| $j$ | = | computer cycle time index for low-speed portion of two-speed attitude updating algorithm |
| $l$ | = | general computer cycle time index; computer cycle time index for single-speed attitude updating algorithm; computer cycle time index for high-speed portion of two-speed attitude updating algorithm |
| $m$, $n$ | = | computer cycle time indices for velocity and position updating |
| $\boldsymbol{n}_P$ | = | vector of independent white process noise components |
| $Q_{\alpha\psi}$, $Q_{\alpha\psi v}$ | = | white noise spectral density matrices associated with $\delta\boldsymbol{\alpha}_{\psi_{\text{quant}}}$ and $\delta\boldsymbol{\alpha}_{\psi v_{\text{quant}}}$ |
| $Q_{vR}$, $Q_{vvR}$ | = | white noise spectral density matrices associated with $\delta\boldsymbol{v}_{R_{\text{quant}}}$ and $\delta\boldsymbol{v}_{vR_{\text{quant}}}$ |
| $\boldsymbol{R}^I$ | = | position vector from Earth's center to the navigation system projected on $I$ frame axes |
| $r$ | = | ratio of the $l$ cycle attitude update frequency over the $m$ cycle velocity update frequency (assuming that $l$ cycle frequency is an integer multiple of the $m$ cycle frequency) |
| $s$ | = | ratio of the $m$ cycle velocity update frequency over the $n$ cycle position update frequency (assuming that $m$ cycle frequency is an integer multiple of the $n$ cycle frequency) |

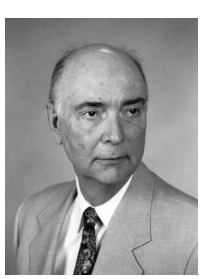

**Paul G. Savage is President of Strapdown Associates, Inc. (www.strapdownassociates.com), a company he founded in 1980 that provides strapdown inertial system design, consulting, and educational services. Since 1981, Mr. Savage has provided his Introduction to Strapdown Inertial Navigation Systems course to the aerospace industry. He has recently written and published the textbook *Strapdown Analytics*. From 1963 to 1980 he was employed at Honeywell, where he led design teams in the evolutionary development of laser gyro strapdown inertial navigation systems. He is a graduate of the Massachusetts Institute of Technology, where in 1960 he received his M.S. and B.S. degrees in aeronautical engineering. He is a Senior Member of AIAA.**

Received 28 January 2002; revision received 15 May 2002; accepted for publication 15 May 2002. 

$u_{\alpha_{\text{quant}}}$ = variance about the mean of the angular rate sensor pulse quantization noise uncertainty; identical to $\mathcal{E}(\chi_\alpha^2) = \varepsilon_\alpha^2/12$

$V_{M_\alpha}$, $V_{M_\upsilon}$ = covariances of the $\boldsymbol{\chi}_\alpha$ and $\boldsymbol{\chi}_\upsilon$ attitude/velocity quantization measurement noise vectors

$\boldsymbol{v}^I$ = velocity (rate of change of the position vector $\boldsymbol{R}$) relative to nonrotating inertial space (i.e., the $I$ frame) as projected on $I$ frame axes

$\boldsymbol{x}$ = error state vector

$\alpha_l$ = integrated angular rate from time $l-1$ to $l$

$\Delta t_l$, $\Delta t_m$, $\Delta t_n$ = time intervals for the $l$, $m$, and $n$ attitude, velocity, and position computer update cycles

$\Delta\boldsymbol{\psi}_l^{I_*}$, $\Delta\boldsymbol{\psi}_m^{I_*}$ = change in $\boldsymbol{\psi}^{I_*}$ over an $l$ and $m$ cycle

$\delta(\,)$ = error in $(\,)$

$\delta\boldsymbol{a}_{\text{quant}}$ = accelerometer output quantization random error vector

$\delta\boldsymbol{a}_{\text{rand}}$ = accelerometer output white noise error vector (integral known as random walk on velocity)

$\delta\boldsymbol{a}_{\text{sf}}^B$ = accelerometer output error vector in $B$ frame coordinates

$\delta\boldsymbol{a}_{\text{sf}}^{B_*}$ = $\delta\boldsymbol{a}_{\text{sf}}^B$ exclusive of accelerometer quantization error

$\delta K_{\text{scal/mis}}$ = angular rate sensor output scale-factor/misalignment error matrix

$\delta\boldsymbol{K}_{\text{bias}}$ = angular rate sensor output bias error vector

$\delta L_{\text{scal/mis}}$ = accelerometer output scale-factor/misalignment error matrix

$\delta\boldsymbol{L}_{\text{bias}}$ = accelerometer output bias error vector

$\delta\boldsymbol{R}_{(\,)}^I$ = $\delta\boldsymbol{R}^I$ at computer cycle $(\,)$

$\delta\boldsymbol{v}_{(\,)}^I$, $\delta\boldsymbol{v}_{(\,)}^{I_*}$ = $\delta\boldsymbol{v}^I$, $\delta\boldsymbol{v}^{I_*}$ at computer cycle $(\,)$

$\delta\boldsymbol{v}^{I_*}$ = revised form of $\delta\boldsymbol{v}^I$ that neglects the instantaneous $C_B^I\delta\boldsymbol{\upsilon}_{\text{quant}}$ part of the $\delta\boldsymbol{v}^I$ quantization error [from Eq. (34), parameter still contains accelerometer quantization error input under applied angular rates]

$\delta\alpha_{\text{quant}_l}$ = angular rate sensor integrated rate increment quantization error for computer cycle $l$

$\delta\boldsymbol{\alpha}_l$ = defined by Eq. (46)

$\delta\boldsymbol{\alpha}_l^*$ = $\delta\boldsymbol{\alpha}_l$ exclusive of sensor quantization error

$\delta\boldsymbol{\alpha}_{\text{quant}}$ = angular rate sensor white noise quantization error associated with the integral of angular rate sensor outputs

$\delta\boldsymbol{\alpha}_{\text{quant}_l}$ = quantization error vector contribution to $\delta\boldsymbol{\alpha}_l$

$\delta\boldsymbol{\alpha}_{\psi_{\text{quant}}}$, $\delta\boldsymbol{\alpha}_{\psi\upsilon_{\text{quant}}}$ = white quantization noise vector equivalents to $\boldsymbol{\zeta}_{\alpha\psi_m}$ and $\boldsymbol{\chi}_{\alpha\psi\upsilon_m}$

$\delta\boldsymbol{\upsilon}_m$ = defined by Eq. (42)

$\delta\boldsymbol{\upsilon}_m^*$ = $\delta\boldsymbol{\upsilon}_m$ exclusive of sensor quantization error

$\delta\boldsymbol{\upsilon}_{\text{quant}}$ = accelerometer white noise quantization error associated with the integral of accelerometer outputs

$\delta\boldsymbol{\upsilon}_{\text{quant}_m}$ = quantization error vector contribution to $\delta\boldsymbol{\upsilon}_m$

$\delta\boldsymbol{\upsilon}_{\upsilon_{\text{quant}}}$, $\delta\boldsymbol{\upsilon}_{\upsilon R_{\text{quant}}}$ = independent accelerometer white noise quantization noise vectors equivalent to $\delta\boldsymbol{\alpha}_{\psi_{\text{quant}}}$ and $\delta\boldsymbol{\alpha}_{\psi\upsilon_{\text{quant}}}$ for angular rate sensors

$\delta\boldsymbol{\omega}_{\text{quant}}$ = angular rate sensor output quantization random error vector

$\delta\boldsymbol{\omega}_{\text{rand}}$ = angular rate sensor output white noise error vector (integral known as random walk on attitude)

$\delta\boldsymbol{\omega}^B$ = angular rate sensor output error vector in $B$ frame coordinates

$\delta\boldsymbol{\omega}^{B_*}$ = $\delta\boldsymbol{\omega}^B$ exclusive of angular rate sensor quantization error

$\varepsilon_\alpha$ = angular rate sensor output pulse size

$\varepsilon_\upsilon$ = accelerometer output pulse size

$\boldsymbol{\zeta}_{\alpha\psi_m}$ = cumulative angular rate sensor pulse quantization error over an $m$ cycle (exclusive of the $\boldsymbol{\chi}_{\alpha\psi\upsilon_m}$ error), which appears only in the attitude error equation

$\xi_{\alpha_l}$ = instantaneous angular rate sensor quantization error at computer cycle $l$

$\boldsymbol{\phi}_j^{B_{j-1}}$, $\boldsymbol{\phi}_l^{B_{j-1}}$ = $\boldsymbol{\phi}^{B_{j-1}}$ at computer cycles $j$ and $l$

$\boldsymbol{\phi}^{B_{j-1}}$ = misalignment error angle vector associated with $\hat{C}_B^{B_{j-1}}$ in $B_{j-1}$ frame coordinates, considering the $B_{j-1}$ frame to be misaligned relative to the $B$ frame

$\chi_{\alpha_l}$ = instantaneous angular rate sensor random quantization error at cycle $l$ having a value between $-\varepsilon_\alpha/2$ and $+\varepsilon_\alpha/2$ with equal probability (i.e., uniformly distributed)

$\boldsymbol{\chi}_{\alpha_l}$, $\boldsymbol{\chi}_{\upsilon_m}$ = angular rate sensor and accelerometer quantization error vectors at update times $l$ and $m$

$\boldsymbol{\chi}_{\alpha\psi\upsilon_m}$ = angular rate sensor pulse quantization error that occurs once each $m$ cycle in both the attitude and velocity error equations

$\boldsymbol{\psi}^I$ = misalignment error angle vector associated with $\hat{C}_B^I$ in $I$ frame coordinates, considering the $I$ frame to be misaligned relative to the $B$ frame

$\boldsymbol{\psi}^{I_*}$ = revised form of $\boldsymbol{\psi}^I$ that neglects the instantaneous $C_B^I\delta\boldsymbol{\alpha}_{\text{quant}}$ part of the $\boldsymbol{\psi}^I$ quantization error [from Eq. (28), parameter still contains cumulative angular rate sensor quantization error effects under applied angular rates]

$\boldsymbol{\psi}_{(\,)}^I$, $\boldsymbol{\psi}_{(\,)}^{I_*}$ = $\boldsymbol{\psi}^I$, $\boldsymbol{\psi}^{I_*}$ at computer cycle $(\,)$

$\boldsymbol{\omega}^B$ = sensor assembly angular rate vector relative to nonrotating inertial space as projected on $B$ frame axes (i.e., angular rate sensed by strapdown angular rate sensors)

$(\,)\times$ = skew symmetric cross-product form of the $(\,)$ vector;[5,6]

$\hat{(\,)}$ = value for $(\,)$ calculated in the strapdown system computer error; parameter without caret is considered nominal error free value

## Introduction

In many strapdown inertial navigation systems, the inertial sensor outputs (from angular rate sensors and accelerometers) represent integrated samples of the sensor inputs over each system computer navigation parameter update cycle. In practice, this is achieved by counting output pulses from the sensors during each update cycle. Each sensor pulse represents the occurrence of a specified increment of integrated sensor input. One can imagine the attitude and velocity parameters in the strapdown computer being generated as a repetitive summing operation on the sensor count samples. For perfect inertial sensors, the complete integrals, that is, attitude and velocity, so generated will be correct, but only to within a pulse because the instantaneous pulse output will, in general, not occur exactly at the computer sample time instant. The associated error effect is called pulse quantization.

Integration algorithms in the strapdown computer process the sensor outputs to continuously calculate attitude, velocity, and position navigation parameters. Because of errors in the sensor outputs, the navigation parameters develop error buildup with time. Error equations associated with strapdown inertial systems generally describe navigation parameter error propagation characteristics in response to initial uncertainties and inertial sensor errors. Typical sensor error models have included scale factor, misalignment, bias errors, and sensor-induced random output noise, with the random noise modeled as white process noise such that its integral gives rise to a "random walk" (i.e., random walk on attitude for angular rate

sensors and random walk on velocity for accelerometers). Sensor quantization represents an additional random error source that usually has less impact on system inaccuracy than the random-walk-type noise. As such, it is often neglected altogether[1–3] or included as part of random walk noise. For incremental integrating sensors such as described earlier, the latter random walk modeling approximation is incorrect and can lead to erroneously large growth rates in system error parameter propagation equations.

This paper develops an analytical model for inertial sensor quantization noise and how it can be properly represented in strapdown inertial system attitude, velocity, and position error equations. The model is useful for assessing the magnitude of quantization noise-induced system error and if significant, how to include it in system navigation parameter error propagation and measurement equations. System error propagation models are developed both as continuous form differential equations and as discrete difference equations. For each, it is shown how the attitude, velocity, and sensor error parameters must be modified to enable proper quantization error modeling as white noise for compatibility with standard error state dynamic equation formatting.

The discrete form system error propagation model is used to develop analytical expressions for attitude/velocity measurement quantization noise covariances and for spectral densities of white quantization noise terms in the differential error propagation equations. These include correlations that exist between attitude and velocity errors from angular rate sensor quantization noise inputs, and between velocity and position error from accelerometer quantization noise inputs. The discrete difference form also reveals that the continuous form error propagation equation derivation implicitly assumed equal attitude, velocity, and position parameter update frequencies in the strapdown system computer, and how the continuous form error equations should be modified for the general case of different navigation parameter update frequencies.

A general discussion is provided of how quantization white noise spectral densities should be computed for compatibility with two-speed attitude, velocity, and position updating algorithms. The paper includes examples illustrating the computation of numerical values for quantization noise effects and how incorrect modeling can lead to significant mischaracterization of the effect of quantization noise on system accuracy. Validity regions are discussed regarding modeling quantization error as random noise. Finally, compensation techniques are described for reducing quantization error if necessary to meet system accuracy requirements.

The material presented in this paper is a composite and extension of material originally presented in Ref. 4.

## Sensor Quantization Error Model

An analytical model for quantization error can be developed (Ref. 4, pp. 18-119–18-120) by considering how integrated sensor output increments are formed as the summing of pulses in the system computer from the end of navigation parameter update cycle $l-1$ to the end of cycle $l$. Imagine a situation in which the pulse count from the $l-1$ cycle time happened to begin instantaneously after a pulse was emitted ("start" pulse). For an angular rate sensor, the pulse count from this time forward would be a true indication of integrated angular rate (i.e., attitude change) at any instant that a pulse has been received and counted. Now consider that the $l-1$ cycle time pulse count is initiated a small time interval before the start pulse, in which the small time interval is less than the local time interval between pulses (Fig. 1). The first pulse that is counted (i.e., the start pulse) will be in error (a quantization error) because it is registered as a full pulse when in fact the time period for the count was less than a full pulse period. The maximum error under this condition occurs when a pulse is received (and counted) instantaneously after the $l-1$ time instant and will equal one pulse. Thus, the quantization error introduced at $l-1$ can range in magnitude from zero to one pulse with a mean value of half a pulse (for a uniform statistical quantization error distribution). The sign of the quantization error will be the sign of the instantaneous pulse rate (positive or negative). The pulse count from this point forward will add no additional quantization error until the $l$ cycle is reached to halt the incremental count.

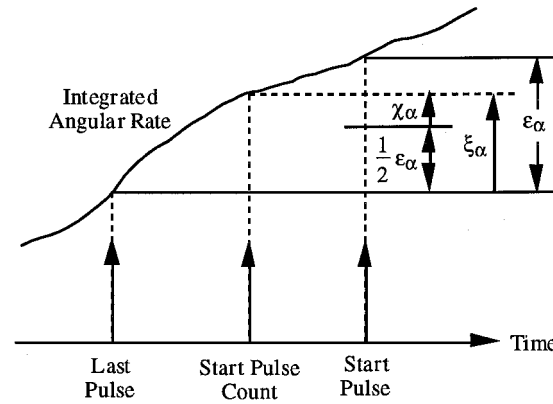


**Fig. 1 Start of pulse count sampling.**

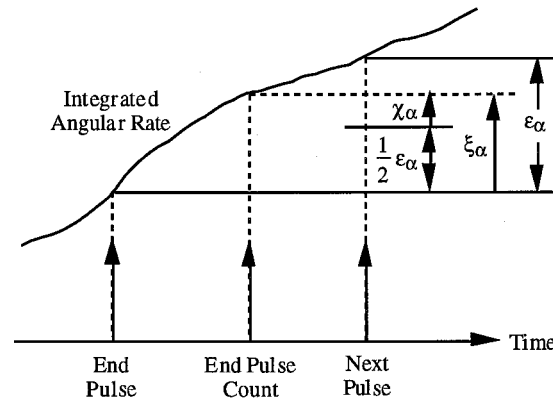


**Fig. 2 End of pulse count sampling.**

If the count is halted at a finite time interval following a pulse occurrence ("end" pulse), the pulse count at $l$ will experience an additional quantization error because the integrated angular rate since the end pulse has not been registered in the count (Fig. 2). The error will be maximum at one pulse magnitude if the count is halted at the instant before receipt of the next pulse. Thus, the added quantization error at $l$ will be in the range of zero to minus one pulse with a mean value of minus half a pulse. The sign of the error in this case will be the negative of the instantaneous pulse rate at $l$.

The preceding discussion is the basis for the following angular rate sensor pulse count quantization error model:

$$\delta\alpha_{\text{quant}_l} = \xi_{\alpha_l} - \xi_{\alpha_{l-1}}, \qquad \xi_{\alpha_l} = (\varepsilon_\alpha/2)\,\text{sign}(\alpha_l) + \chi_{\alpha_l} \tag{1}$$

We assume that, for the most part, $\delta\alpha_{\text{quant}_l}$ will have the same sign at cycle $l-1$ and $l$ so that Eqs. (1) when combined yield

$$\delta\alpha_{\text{quant}_l} = \chi_{\alpha_l} - \chi_{\alpha_{l-1}} \tag{2}$$

From Eq. (2), we see that the cumulative error in the sum of the angular rate sensor incremental pulse count increments (i.e., the error in the integrated angular rate) is given by

$$\sum_{l=1}^{L} \delta\alpha_{\text{quant}_l} = \chi_{\alpha_L} - \chi_{\alpha_1} \tag{3}$$

The $\chi_{\alpha_1}$ term in Eq. (3) can be considered to be an initialization error on the integrated angular rate; the $\chi_{\alpha_L}$ term is a random error on the integrated rate at cycle time $L$. Thus, Eq. (3) shows that quantization noise can be modeled as random noise on the integrated inertial sensor output signal.

## Strapdown Sensor Generic Error Models

Strapdown inertial sensor errors can be represented by the following vector forms (Ref. 4, pp. 12-110, 12-111):

$$\delta\boldsymbol{\omega}^B = \delta K_{\text{scal/mis}}\boldsymbol{\omega}^B + \delta\boldsymbol{K}_{\text{bias}} + \delta\boldsymbol{\omega}_{\text{rand}} + \delta\boldsymbol{\omega}_{\text{quant}} \tag{4}$$

$$\delta\boldsymbol{a}^B_{\text{sf}} = \delta L_{\text{scal/mis}}\boldsymbol{a}^B_{\text{sf}} + \delta\boldsymbol{L}_{\text{bias}} + \delta\boldsymbol{a}_{\text{rand}} + \delta\boldsymbol{a}_{\text{quant}} \tag{5}$$

The $\delta\boldsymbol{\omega}_{\text{quant}}$ and $\delta\boldsymbol{a}_{\text{quant}}$ quantization error terms in Eqs. (4) and (5) represent random errors on the direct (not integrated) sensor

outputs. The discussion in the preceding section showed that quantization error can be accurately modeled as a white uniform random error process on each integrated sensor output. Hence, $\delta\boldsymbol{\omega}_{\text{quant}}$ and $\delta\boldsymbol{a}_{\text{quant}}$ represent the time derivative of the white random quantization error process associated with the integrated output. Because a white uniform random process on the integrated sensor outputs is easily defined mathematically, it is expeditious to substitute for $\delta\boldsymbol{\omega}_{\text{quant}}$ and $\delta\boldsymbol{a}_{\text{quant}}$ (Ref. 4, p. 12-113):

$$\delta\boldsymbol{\omega}_{\text{quant}} = \delta\dot{\boldsymbol{\alpha}}_{\text{quant}}, \qquad \delta\boldsymbol{a}_{\text{quant}} = \delta\dot{\boldsymbol{\upsilon}}_{\text{quant}} \tag{6}$$

## Strapdown Inertial Navigation Differential Equations

To analyze how quantization noise is properly modeled in typical strapdown inertial navigation systems we will study its effect on a representative set of the differential equations implemented by integration algorithms in the system computer. To simplify the analysis, the equations will be written for a nonrotating "inertial" coordinate frame with position location represented as a position vector, in contrast with more traditional but analytically equivalent methods in which equations are written in a locally level rotating coordinate frame (e.g., wander azimuth) and position location is represented by altitude and angular location over the Earth's surface (Ref. 4, pp. 4-3–4-8, 4-10–4-14, and 4-16–4-20). Error modeling methods to be presented are comparable for either coordinate frame approach. With the use of Refs. 4 (pp. 12-21–12-23), 5, 6, and 7 (pp. 16, 17) as guides, we write the strapdown navigation equations as

$$\dot{C}_B^I = C_B^I(\boldsymbol{\omega}^B\times) \tag{7}$$

$$\dot{\boldsymbol{v}}^I = C_B^I\boldsymbol{a}_{\text{sf}}^B + \boldsymbol{g}^I \tag{8}$$

$$\dot{\boldsymbol{R}}^I = \boldsymbol{v}^I \tag{9}$$

## Strapdown Inertial Navigation Differential Error Propagation Equations

The error rate equations associated with Eqs. (7–9) are obtained from their differential (Ref. 4, pp. 12-65–12-70):

$$\delta\dot{C}_B^I = \delta C_B^I(\boldsymbol{\omega}^B\times) + C_B^I(\delta\boldsymbol{\omega}^B\times) \tag{10}$$

$$\delta\dot{\boldsymbol{v}}^I = \delta C_B^I\boldsymbol{a}_{\text{sf}}^B + C_B^I\delta\boldsymbol{a}_{\text{sf}}^B + \delta\boldsymbol{g}^I \tag{11}$$

$$\delta\dot{\boldsymbol{R}}^I = \delta\boldsymbol{v}^I \tag{12}$$

We assume that through proper software design practices, there will be no significant orthogonality or normality errors in the system computed value of $C_B^I$. Then the error in computed $C_B^I$ can be attributed entirely to misalignment, which we characterize in traditional fashion [Refs. 4 (pp. 3-78–3-79) and 7 (p. 164)] as

$$\hat{C}_B^I = [\mathrm{I} - (\boldsymbol{\psi}^I\times)]C_B^I \tag{13}$$

Using the definition for $\delta C_B^I$ and substituting (13) then finds

$$\delta C_B^I \equiv \hat{C}_B^I - C_B^I = -(\boldsymbol{\psi}^I\times)C_B^I \tag{14}$$

The derivative of Eq. (14) with Eq. (7) is

$$\delta\dot{C}_B^I = -(\dot{\boldsymbol{\psi}}^I\times)C_B^I - (\boldsymbol{\psi}^I\times)\dot{C}_B^I = -(\dot{\boldsymbol{\psi}}^I\times)C_B^I - (\boldsymbol{\psi}^I\times)C_B^I(\boldsymbol{\omega}^B\times) \tag{15}$$

Substituting Eqs. (14) and (15) in Eq. (10) obtains, with rearrangement,

$$(\dot{\boldsymbol{\psi}}^I\times) = -C_B^I(\delta\boldsymbol{\omega}^B\times)\left(C_B^I\right)^T = -\left[\left(C_B^I\delta\boldsymbol{\omega}^B\right)\times\right] \tag{16}$$

or equivalently,

$$\dot{\boldsymbol{\psi}}^I = -C_B^I\delta\boldsymbol{\omega}^B \tag{17}$$

Finally, we substitute Eqs. (4–6) for $\delta\boldsymbol{\omega}^B$ and $\delta\boldsymbol{a}_{\text{sf}}^B$ in Eqs. (17) and (11), substitute Eq. (14) for $\delta C_B^I$ in the revised $\delta\dot{\boldsymbol{v}}^I$ equation, recognize that $(\boldsymbol{\psi}^I\times)C_B^I\boldsymbol{a}_{\text{sf}}^B = \boldsymbol{\psi}^I\times\boldsymbol{a}_{\text{sf}}^I = -\boldsymbol{a}_{\text{sf}}^I\times\boldsymbol{\psi}^I$, and with Eq. (12) summarize results:

$$\dot{\boldsymbol{\psi}}^I = -C_B^I\left(\delta K_{\text{scal/mis}}\boldsymbol{\omega}^B + \delta\boldsymbol{K}_{\text{bias}} + \delta\boldsymbol{\omega}_{\text{rand}} + \delta\dot{\boldsymbol{\alpha}}_{\text{quant}}\right) \tag{18}$$

$$\delta\dot{\boldsymbol{v}}^I = \boldsymbol{a}_{\text{sf}}^I\times\boldsymbol{\psi}^I + C_B^I\left(\delta L_{\text{scal/mis}}\boldsymbol{a}_{\text{sf}}^B + \delta\boldsymbol{L}_{\text{bias}} + \delta\boldsymbol{a}_{\text{rand}} + \delta\dot{\boldsymbol{\upsilon}}_{\text{quant}}\right) + \delta\boldsymbol{g}^I \tag{19}$$

$$\delta\dot{\boldsymbol{R}}^I = \delta\boldsymbol{v}^I \tag{20}$$

Equations (18–20) constitute the error form of strapdown inertial equations (7–9) in which the noise terms (rand and quant subscripted) are modeled as white noise. A fundamental problem exists with these equations if they are to be used for classical error state vector formulations; quantization noise terms appear as their derivatives which is incompatible with standard error state dynamic equation format [Refs. 4 (p. 15-2), 8, and 9]:

$$\dot{\boldsymbol{x}} = A\boldsymbol{x} + G_P\boldsymbol{n}_P \tag{21}$$

The following section shows how Eqs. (18–20) can be modified into the standard Eq. (21) format.

## Error Equation Revisions to Enhance Quantization Noise Modeling

We begin by revising attitude error equation (18) as follows (Ref. 4, pp. 12-113–12-115):

$$\dot{\boldsymbol{\psi}}^I + C_B^I\delta\dot{\boldsymbol{\alpha}}_{\text{quant}} = -C_B^I\left(\delta K_{\text{scal/mis}}\boldsymbol{\omega}^B + \delta\boldsymbol{K}_{\text{bias}} + \delta\boldsymbol{\omega}_{\text{rand}}\right) \tag{22}$$

and note that

$$C_B^I\delta\dot{\boldsymbol{\alpha}}_{\text{quant}} = \frac{\mathrm{d}}{\mathrm{dt}}\left(C_B^I\delta\boldsymbol{\alpha}_{\text{quant}}\right) - \dot{C}_B^I\delta\boldsymbol{\alpha}_{\text{quant}} \tag{23}$$

so that Eq. (22) is equivalently

$$\frac{\mathrm{d}}{\mathrm{dt}}\left(\boldsymbol{\psi}^I + C_B^I\delta\boldsymbol{\alpha}_{\text{quant}}\right) = -C_B^I\left(\delta K_{\text{scal/mis}}\boldsymbol{\omega}_{IB}^B + \delta\boldsymbol{K}_{\text{bias}} + \delta\boldsymbol{\omega}_{\text{rand}}\right) + \dot{C}_B^I\delta\boldsymbol{\alpha}_{\text{quant}} \tag{24}$$

The form of Eq. (24) suggests the definition of revised attitude and angular rate sensor error parameters:

$$\boldsymbol{\psi}^{I_*} \equiv \boldsymbol{\psi}^I + C_B^I\delta\boldsymbol{\alpha}_{\text{quant}} \tag{25}$$

$$\delta\boldsymbol{\omega}^{B_*} \equiv \delta K_{\text{scal/mis}}\boldsymbol{\omega}_{IB}^B + \delta\boldsymbol{K}_{\text{bias}} + \delta\boldsymbol{\omega}_{\text{rand}} \tag{26}$$

The converse of Eq. (24) will also be useful,

$$\boldsymbol{\psi}^I = \boldsymbol{\psi}^{I_*} - C_B^I\delta\boldsymbol{\alpha}_{\text{quant}} \tag{27}$$

Substituting Eqs. (25) and (26) in Eq. (24) with Eq. (7) for $\dot{C}_B^I$ then yields the final form:

$$\dot{\boldsymbol{\psi}}^{I_*} = -C_B^I\delta\boldsymbol{\omega}^{B_*} + C_B^I(\boldsymbol{\omega}^B\times)\delta\boldsymbol{\alpha}_{\text{quant}} \tag{28}$$

The identical procedure is applied to the velocity and accelerometer error terms in Eq. (19), namely,

$$\delta\boldsymbol{v}^{I_*} \equiv \delta\boldsymbol{v}^I - C_B^I\delta\boldsymbol{\upsilon}_{\text{quant}} \tag{29}$$

$$\delta\boldsymbol{a}_{\text{sf}}^{B_*} \equiv \delta L_{\text{scal/mis}}\boldsymbol{a}_{\text{sf}}^B + \delta\boldsymbol{L}_{\text{bias}} + \delta\boldsymbol{a}_{\text{rand}} \tag{30}$$

$$\delta\boldsymbol{v}^I = \delta\boldsymbol{v}^{I_*} + C_B^I\delta\boldsymbol{\upsilon}_{\text{quant}} \tag{31}$$

The derivative of Eq. (29) is

$$\delta\dot{\boldsymbol{v}}^{I_*} = \delta\dot{\boldsymbol{v}}^I - \dot{C}_B^I\delta\boldsymbol{\upsilon}_{\text{quant}} - C_B^I\delta\dot{\boldsymbol{\upsilon}}_{\text{quant}} \tag{32}$$

In Eq. (32), we then substitute Eq. (19) for $\delta\dot{\boldsymbol{v}}^I$ and Eq. (7) for $\dot{C}_B^I$; in the result, substitute Eq. (27) for $\boldsymbol{\psi}^I$; recognize that

$$\left(\boldsymbol{a}_{\text{sf}}^I \times\right) C_B^I \delta\boldsymbol{\alpha}_{\text{quant}} = C_B^I \left(C_B^I\right)^T \left(\boldsymbol{a}_{\text{sf}}^I \times\right) C_B^I \delta\boldsymbol{\alpha}_{\text{quant}}$$
$$= C_B^I \left(\boldsymbol{a}_{\text{sf}}^B \times\right) \delta\boldsymbol{\alpha}_{\text{quant}}$$

and apply the equation (30) $\delta\boldsymbol{a}_{\text{sf}}^{B_*}$ accelerometer error definition. Last, we substitute Eq. (31) for $\delta\boldsymbol{v}^I$ in the equation (20) $\delta\dot{\boldsymbol{R}}^I$ expression, and with Eq. (28), summarize results:

$$\dot{\boldsymbol{\psi}}^{I_*} = -C_B^I \delta\boldsymbol{\omega}^{B_*} + C_B^I (\boldsymbol{\omega}^B \times) \delta\alpha_{\text{quant}} \tag{33}$$

$$\delta\dot{\boldsymbol{v}}^{I_*} = \boldsymbol{a}_{\text{sf}}^I \times \boldsymbol{\psi}^{I_*} + C_B^I \delta\boldsymbol{a}_{\text{sf}}^{B_*} + \delta\boldsymbol{g}^I$$
$$- C_B^I \left(\boldsymbol{a}_{\text{sf}}^B \times\right) \delta\boldsymbol{\alpha}_{\text{quant}} - C_B^I (\boldsymbol{\omega}^B \times) \delta\boldsymbol{\upsilon}_{\text{quant}} \tag{34}$$

$$\delta\dot{\boldsymbol{R}}^I = \delta\boldsymbol{v}^{I_*} + C_B^I \delta\boldsymbol{\upsilon}_{\text{quant}} \tag{35}$$

Equations (33–35) with Eqs. (26), (27), (30), and (31) constitute a complete consistent set for the new (and old) variables $\boldsymbol{\psi}^{I_*}$, $\boldsymbol{\psi}^I$, $\delta\boldsymbol{v}^{I_*}$, $\delta\boldsymbol{v}^I$, and $\delta\boldsymbol{R}^I$. Propagation equations (33–35) only contain direct white noise terms, that is, no white noise derivatives, hence, are compatible with the standard Eq. (21) format. These equations can be used in place of navigation error equations (18–20) for the $\boldsymbol{\psi}^I$, $\delta\boldsymbol{v}^I$, and $\delta\boldsymbol{R}^I$ error parameters.

Recognize that although Eqs. (33–35) were configured to enhance white noise modeling of sensor quantization errors, their derivation never explicitly assumed that quantization error was white noise. Consequently, these equations are general and equally valid for any representation of quantization error that may exist under particular sensor input situations. This point will be discussed further at the end of the paper.

When Eqs. (27), (31), and (33–35) quantization errors are modeled as white noise, their numerical characterization is classically described in terms of statistical covariances or white noise spectral densities. To relate the noise values to the sensor quantization noise model (see "Sensor Quantization Error Model" section) we will need the equivalent discrete difference form of Eqs. (33–35) as derived in the next section.

## Equivalent Discrete Difference Error Equation Forms

The discrete difference equivalent to differential equations (7–9) at the attitude, velocity, and position updating algorithm computer cycle times is

$$C_{B_l}^I = C_{B_{l-1}}^I C_{B_l}^{B_{l-1}} \tag{36}$$

$$\boldsymbol{v}_m^I = \boldsymbol{v}_{m-1}^I + C_{B_{m-1}}^I \int_{t_{m-1}}^{t_m} C_B^{B_{m-1}} \boldsymbol{a}_{\text{sf}}^B \, \text{d}t + \boldsymbol{g}_m^I \Delta t_m \tag{37}$$

$$\boldsymbol{R}_n^I = \boldsymbol{R}_{n-1}^I + \boldsymbol{v}_{n-1}^I \Delta t_n + \int_{t_{n-1}}^{t_n} \left(\boldsymbol{v}^I - \boldsymbol{v}_{n-1}^I\right) \text{d}t \tag{38}$$

Figure 3 illustrates a typical timing relationship between the Eq. (36–38) attitude, velocity, and position update cycles.

When it is assumed that the computer update rate is fast enough that $B$ frame orientations between times $m-1$ and $m$ are close to one another, the error form (differential) of Eqs. (36–38) is

$$\delta C_{B_l}^I = \delta C_{B_{l-1}}^I C_{B_l}^{B_{l-1}} + C_{B_{l-1}}^I \delta C_{B_l}^{B_{l-1}} \tag{39}$$

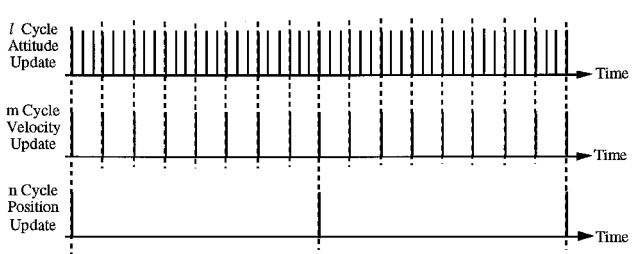


**Fig. 3 Computation timing cycle pulses.**

$$\delta\boldsymbol{v}_m^I = \delta\boldsymbol{v}_{m-1}^I + \delta C_{B_{m-1}}^I \int_{t_{m-1}}^{t_m} C_B^{B_{m-1}} \boldsymbol{a}_{\text{sf}}^B \, \text{d}t$$
$$+ C_{B_{m-1}}^I \delta\left(\int_{t_{m-1}}^{t_m} C_B^{B_{m-1}} \boldsymbol{a}_{\text{sf}}^B \, \text{d}t\right) + \delta\boldsymbol{g}_m^I \Delta t_m \approx \delta\boldsymbol{v}_{m-1}^I$$
$$+ \delta C_{B_{m-1}}^I \int_{t_{m-1}}^{t_m} \boldsymbol{a}_{\text{sf}}^B \, \text{d}t + C_{B_{m-1}}^I \delta\left(\int_{t_{m-1}}^{t_m} \boldsymbol{a}_{\text{sf}}^B \, \text{d}t\right) + \delta\boldsymbol{g}_m^I \Delta t_m$$
$$= \delta\boldsymbol{v}_{m-1}^I + \delta C_{B_{m-1}}^I \boldsymbol{\upsilon}_m + C_{B_{m-1}}^I \delta\boldsymbol{\upsilon}_m + \delta\boldsymbol{g}_m^I \Delta t_m \tag{40}$$

$$\delta\boldsymbol{R}_n^I = \delta\boldsymbol{R}_{n-1}^I + \delta\boldsymbol{v}_{n-1}^I \Delta t_n + \int_{t_{n-1}}^{t_n} \delta\left(\boldsymbol{v}^I - \boldsymbol{v}_{n-1}^I\right) \text{d}t$$
$$\approx \delta\boldsymbol{R}_{n-1}^I + \delta\boldsymbol{v}_{n-1}^I \Delta t_n \tag{41}$$

with

$$\boldsymbol{\upsilon}_m \equiv \int_{t_{m-1}}^{t_m} \boldsymbol{a}_{\text{sf}}^B \, \text{d}t, \qquad \delta\boldsymbol{\upsilon}_m = \int_{t_{m-1}}^{t_m} \delta\boldsymbol{a}_{\text{sf}}^B \, \text{d}t \tag{42}$$

Substituting Eq. (14) in Eqs. (39) and (40) finds

$$-\left(\boldsymbol{\psi}_l^I \times\right) C_{B_l}^I = -\left(\boldsymbol{\psi}_{l-1}^I \times\right) C_{B_{l-1}}^I C_{B_l}^{B_{l-1}} + C_{B_{l-1}}^I \delta C_{B_l}^{B_{l-1}}$$
$$= -\left(\boldsymbol{\psi}_{l-1}^I \times\right) C_{B_l}^I + C_{B_{l-1}}^I \delta C_{B_l}^{B_{l-1}} \tag{43}$$

$$\delta\boldsymbol{v}_m^I = \delta\boldsymbol{v}_{m-1}^I + \left(C_{B_{m-1}}^I \boldsymbol{\upsilon}_m\right) \times \boldsymbol{\psi}_{m-1}^I + C_{B_{m-1}}^I \delta\boldsymbol{\upsilon}_m + \delta\boldsymbol{g}_m^I \Delta t_m \tag{44}$$

In traditional fashion [Refs. 4 (p. 7-37) and 10 (p. 351)], we approximate

$$C_{B_l}^{B_{l-1}} \approx \text{I} + (\boldsymbol{\alpha}_l \times), \qquad \delta C_{B_l}^{B_{l-1}} = (\delta\boldsymbol{\alpha}_l \times) \tag{45}$$

with

$$\boldsymbol{\alpha}_l \equiv \int_{t_{l-1}}^{t_l} \boldsymbol{\omega}^B \, \text{d}t, \qquad \delta\boldsymbol{\alpha}_l = \int_{t_{l-1}}^{t_l} \delta\boldsymbol{\omega}^B \, \text{d}t \tag{46}$$

Multiplying Eq. (43) on the right by $-(C_{B_l}^I)^T$ and substituting Eq. (45) then obtains

$$\left(\boldsymbol{\psi}_l^I \times\right) \approx \left(\boldsymbol{\psi}_{l-1}^I \times\right) - C_{B_{l-1}}^I (\delta\boldsymbol{\alpha}_l \times) \left(C_{B_{l-1}}^I\right)^T$$
$$= \left(\boldsymbol{\psi}_{l-1}^I \times\right) - \left[\left(C_{B_{l-1}}^I \delta\boldsymbol{\alpha}_l\right) \times\right] \tag{47}$$

or

$$\boldsymbol{\psi}_l^I = \boldsymbol{\psi}_{l-1}^I - C_{B_{l-1}}^I \delta\boldsymbol{\alpha}_l \tag{48}$$

Equations (48), (44), and (41) (summarized next) represent discrete difference equivalents to differential error propagation equations (18–20):

$$\boldsymbol{\psi}_l^I = \boldsymbol{\psi}_{l-1}^I - C_{B_{l-1}}^I \delta\boldsymbol{\alpha}_l \tag{49}$$

$$\delta\boldsymbol{v}_m^I = \delta\boldsymbol{v}_{m-1}^I + \left(C_{B_{m-1}}^I \boldsymbol{\upsilon}_m\right) \times \boldsymbol{\psi}_{m-1}^I + C_{B_{m-1}}^I \delta\boldsymbol{\upsilon}_m + \delta\boldsymbol{g}_m^I \Delta t_m \tag{50}$$

$$\delta\boldsymbol{R}_n^I = \delta\boldsymbol{R}_{n-1}^I + \delta\boldsymbol{v}_{n-1}^I \Delta t_n \tag{51}$$

Focusing on the angular rate sensor quantization error portion of $\delta\boldsymbol{\alpha}_l$ and $\delta\boldsymbol{\upsilon}_m$, we define

$$\delta\boldsymbol{\alpha}_l = \delta\boldsymbol{\alpha}_l^* + \delta\boldsymbol{\alpha}_{\text{quant}_l}, \qquad \delta\boldsymbol{\upsilon}_m = \delta\boldsymbol{\upsilon}_m^* + \delta\boldsymbol{\upsilon}_{\text{quant}_m} \tag{52}$$

and based on the vector form of the equation (2) quantization error model for angular rate sensors and accelerometers

$$\delta\boldsymbol{\alpha}_{\text{quant}_l} = \boldsymbol{\chi}_{\alpha_l} - \boldsymbol{\chi}_{\alpha_{l-1}}, \qquad \delta\boldsymbol{\upsilon}_{\text{quant}_m} = \boldsymbol{\chi}_{\upsilon_m} - \boldsymbol{\chi}_{\upsilon_{m-1}} \tag{53}$$

We also define, as in Eqs. (25), (27), (29), and (31),

$$\boldsymbol{\psi}_l^{I^*} \equiv \boldsymbol{\psi}_l^I + C_{B_{l-1}}^I \boldsymbol{\chi}_{\alpha_l}, \qquad \delta \boldsymbol{v}_m^{I_*} = \delta \boldsymbol{v}_m^I - C_{B_{m-1}}^I \boldsymbol{\chi}_{\upsilon_m} \tag{54}$$

$$\boldsymbol{\psi}_l^I = \boldsymbol{\psi}_l^{I^*} - C_{B_{l-1}}^I \boldsymbol{\chi}_{\alpha_l}, \qquad \delta \boldsymbol{v}_m^I = \delta \boldsymbol{v}_m^{I_*} + C_{B_{m-1}}^I \boldsymbol{\chi}_{\upsilon_m} \tag{55}$$

Substituting Eqs. (52), (53), and (55) in Eqs. (49–51) yields

$$\boldsymbol{\psi}_l^{I_*} = \boldsymbol{\psi}_{l-1}^{I_*} - C_{B_{l-1}}^I \delta \boldsymbol{\alpha}_l^* + \left(C_{B_{l-1}}^I - C_{B_{l-2}}^I\right) \boldsymbol{\chi}_{\alpha_{l-1}} \tag{56}$$

$$\begin{aligned} \delta \boldsymbol{v}_m^{I_*} = {} & \delta \boldsymbol{v}_{m-1}^{I_*} + C_{B_{m-1}}^I \delta \boldsymbol{\upsilon}_m^* + \left(C_{B_{m-1}}^I \boldsymbol{\upsilon}_m\right) \times \boldsymbol{\psi}_{m-1}^{I_*} \\ & - \left(C_{B_{m-1}}^I \boldsymbol{\upsilon}_m\right) \times \left(C_{B_{l=r(m-1)-1}}^I \boldsymbol{\chi}_{\alpha_{m-1}}\right) \\ & - \left(C_{B_{m-1}}^I - C_{B_{m-2}}^I\right) \boldsymbol{\chi}_{\upsilon_{m-1}} + \delta g_m^I \Delta t_m \end{aligned} \tag{57}$$

$$\delta \boldsymbol{R}_n^I = \delta \boldsymbol{R}_{n-1}^I + \delta \boldsymbol{v}_{n-1}^{I_*} \Delta t_n + C_{B_{m=s(n-1)-1}}^I \boldsymbol{\chi}_{\upsilon_{n-1}} \Delta t_n \tag{58}$$

From Eqs. (36) and (45), we see that

$$\begin{aligned} C_{B_{l-1}}^I - C_{B_{l-2}}^I &= C_{B_{l-2}}^I (\boldsymbol{\alpha}_{l-1}\times) \\ C_{B_{m-1}}^I - C_{B_{m-2}}^I &= C_{B_{m-2}}^I (\boldsymbol{\alpha}_{m-1}\times) \end{aligned} \tag{59}$$

Then, by recognition that

$$\begin{aligned} & \left(C_{B_{m-1}}^I \boldsymbol{\upsilon}_m\right) \times \left(C_{B_{l=r(m-1)-1}}^I \boldsymbol{\chi}_{\alpha_{m-1}}\right) \\ & \quad \approx C_{B_{m-1}}^I \left(\boldsymbol{\upsilon}_m \times \boldsymbol{\chi}_{\alpha_{m-1}}\right) = C_{B_{m-1}}^I (\boldsymbol{\upsilon}_m \times) \boldsymbol{\chi}_{\alpha_{m-1}} \end{aligned}$$

and that $C_{B_{m=s(n-1)-1}}^I \approx C_{B_{n-1}}^I$, Eqs. (56–58) become the following final forms:

$$\boldsymbol{\psi}_l^{I_*} = \boldsymbol{\psi}_{l-1}^{I_*} - C_{B_{l-1}}^I \delta \boldsymbol{\alpha}_l^* + C_{B_{l-2}}^I (\boldsymbol{\alpha}_{l-1}\times) \boldsymbol{\chi}_{\alpha_{l-1}} \tag{60}$$

$$\begin{aligned} \delta \boldsymbol{v}_m^{I_*} = {} & \delta \boldsymbol{v}_{m-1}^{I_*} + C_{B_{m-1}}^I \delta \boldsymbol{\upsilon}_m^* + \left(C_{B_{m-1}}^I \boldsymbol{\upsilon}_m\right) \times \boldsymbol{\psi}_{m-1}^{I_*} + \delta \boldsymbol{g}_m^I \Delta t_m \\ & - C_{B_{m-1}}^I (\boldsymbol{\upsilon}_m \times) \boldsymbol{\chi}_{\alpha_{m-1}} - C_{B_{m-2}}^I (\boldsymbol{\alpha}_{m-1}\times) \boldsymbol{\chi}_{\upsilon_{m-1}} \end{aligned} \tag{61}$$

$$\delta \boldsymbol{R}_n^I = \delta \boldsymbol{R}_{n-1}^I + \delta \boldsymbol{v}_{n-1}^{I_*} \Delta t_n + C_{B_{n-1}}^I \boldsymbol{\chi}_{\upsilon_{n-1}} \Delta t_n \tag{62}$$

Equations (60–62) with Eq. (55) represent discrete equivalents to continuous form equations (33–35) with Eqs. (27) and (31). Equations (60–62) are used in the next section to develop revised versions of Eqs. (33–35) that properly account for quantization noise coupling between error equations for different navigation parameter update frequencies.

## Revisions to Differential Error Propagation Equations for Proper Quantization Noise Correlation Modeling

For error state dynamic equation modeling, we see from Eqs. (33–35) that angular rate sensor and accelerometer quantization noise $\delta \boldsymbol{\alpha}_{\text{quant}}$ and $\delta \boldsymbol{\upsilon}_{\text{quant}}$ appear in the $\boldsymbol{\psi}^{I_*}$, $\delta \boldsymbol{v}^{I_*}$, and $\delta \boldsymbol{R}$ error propagation continuous form differential equations. Comparing the discrete difference form error propagation equations (60–62) with Eqs. (33–35) shows the equivalency between the $\delta \boldsymbol{\alpha}_{\text{quant}}$, $\delta \boldsymbol{\upsilon}_{\text{quant}}$ continuous form quantization noise parameters, and the $\boldsymbol{\chi}_\alpha$, $\boldsymbol{\chi}_\upsilon$ discrete form parameters. Note from Eqs. (60) and (61) that the $\alpha$ quantization noise terms in the attitude and velocity equations are correlated when the $l$ and $m$ cycles overlap. From Eqs. (61) and (62), we see that a similar correlation exists for the $\upsilon$ quantization noise terms in the velocity and position error equations when the $m$ and $n$ cycles overlap. Proper error state dynamic equation modeling should include these correlation effects. First considering the $\alpha$ angular rate sensor quantization error terms in Eqs. (60) and (61), we write

$$\begin{aligned} \Delta \boldsymbol{\psi}_m^{I_*} &= \sum_{l=r(m-1)+1}^{l=rm} \Delta \boldsymbol{\psi}_l^{I_*} = \cdots + \sum_{l=r(m-1)+1}^{l=rm} C_{B_{l-2}}^I (\boldsymbol{\alpha}_{l-1}\times) \boldsymbol{\chi}_{\alpha_{l-1}} \\ &\approx \cdots + C_{B_{l-2}}^I \left(\boldsymbol{\omega}_{l-1}^B \times\right) \Delta t_l \sum_{l=r(m-1)+1}^{l=rm} \boldsymbol{\chi}_{\alpha_{l-1}} \\ &\approx \cdots + C_{B_m}^I \left(\boldsymbol{\omega}_m^B \times\right) \frac{1}{f_l} \frac{\Delta t_m}{\Delta t_m} \left(\boldsymbol{\chi}_{\alpha_{m-1}} + \sum_{l=r(m-1)+2}^{l=rm} \boldsymbol{\chi}_{\alpha_{l-1}}\right) \\ &= \cdots + \frac{f_m}{f_l} C_{B_m}^I \left(\boldsymbol{\omega}_m^B \times\right) \Delta t_m \left(\boldsymbol{\chi}_{\alpha\psi\upsilon_m} + \boldsymbol{\zeta}_{\alpha\psi_m}\right) \end{aligned}$$

$$\Delta \delta \boldsymbol{v}_m^{I_*} \approx \cdots - C_{B_{m-1}}^I \left(\boldsymbol{a}_{\text{sf}_m}^B \times\right) \Delta t_m \boldsymbol{\chi}_{\alpha\psi\upsilon_m} \tag{63}$$

with

$$\boldsymbol{\chi}_{\alpha\psi\upsilon_m} \equiv \boldsymbol{\chi}_{\alpha_{m-1}}, \qquad \boldsymbol{\zeta}_{\alpha\psi_m} \equiv \sum_{l=r(m-1)+2}^{l=rm} \boldsymbol{\chi}_{\alpha_{l-1}} \tag{64}$$

The equivalent to Eq. (63) on a differential equation basis is the following:

$$\begin{aligned} \dot{\boldsymbol{\psi}}^{I_*} &\approx \frac{\Delta \boldsymbol{\psi}_m^{I_*}}{\Delta t_m} = \cdots + \frac{f_m}{f_l} C_B^I (\boldsymbol{\omega}^B \times) \left(\delta \boldsymbol{\alpha}_{\psi\upsilon_{\text{quant}}} + \delta \boldsymbol{\alpha}_{\psi_{\text{quant}}}\right) \\ \delta \dot{\boldsymbol{v}}^{I_*} &\approx \frac{\Delta \delta \boldsymbol{v}_m^{I_*}}{\Delta t_m} \approx \cdots - C_B^I \left(\boldsymbol{a}_{\text{sf}}^B \times\right) \delta \boldsymbol{\alpha}_{\psi\upsilon_{\text{quant}}} \end{aligned} \tag{65}$$

Similar results apply for the $\upsilon$ accelerometer quantization error terms in Eqs. (61) and (62) compared with Eqs. (34) and (35). We then find, for the composite,

$$\dot{\boldsymbol{\psi}}^{I_*} = -C_B^I \delta \boldsymbol{\omega}^{B_*} + (f_m/f_l) C_B^I (\boldsymbol{\omega}^B \times) \left(\delta \boldsymbol{\alpha}_{\psi\upsilon_{\text{quant}}} + \delta \boldsymbol{\alpha}_{\psi_{\text{quant}}}\right) \tag{66}$$

$$\begin{aligned} \delta \dot{\boldsymbol{v}}^{I_*} = {} & \boldsymbol{a}_{\text{sf}}^I \times \boldsymbol{\psi}^{I_*} + C_B^I \delta \boldsymbol{a}_{\text{sf}}^{B_*} + \delta \boldsymbol{g}^I - C_B^I \left(\boldsymbol{a}_{\text{sf}}^B \times\right) \delta \boldsymbol{\alpha}_{\psi\upsilon_{\text{quant}}} \\ & - (f_n/f_m) C_B^I (\boldsymbol{\omega}^B \times) \left(\delta \boldsymbol{\upsilon}_{\upsilon R_{\text{quant}}} + \delta \boldsymbol{\upsilon}_{\upsilon_{\text{quant}}}\right) \end{aligned} \tag{67}$$

$$\delta \dot{\boldsymbol{R}}^I = \delta \boldsymbol{v}^{I_*} + C_B^I \delta \boldsymbol{\upsilon}_{\upsilon R_{\text{quant}}} \tag{68}$$

Equations (66–68) with Eqs. (26), (30), and (55) are equivalent to Eqs. (33–35) with Eqs. (26), (27), (30), and (31) for the general case when attitude, velocity, and position update frequencies are different. For the case when the $l$ and $m$ update frequencies are equal (i.e., $r = 1$) Eqs. (63) and (64) show that from its definition, $\boldsymbol{\zeta}_{\alpha\psi_m}$ is zero; hence, from its definition, $\delta \boldsymbol{\alpha}_{\psi_{\text{quant}}}$ in Eq. (66) is zero. Similarly, $\delta \boldsymbol{\upsilon}_{\upsilon_{\text{quant}}}$ is zero when the $m$ and $n$ update frequencies are equal. Thus, for equal $l$, $m$, and $n$ update frequencies, Eqs. (66–68) reduce to Eqs. (33–35). Without realizing it then, the derivation of Eqs. (33–35) implicitly assumed equal attitude, velocity, and position update frequencies, which may or may not be the case. In Ref. 4, pp. 16-33–16-34, this point was missed because the more rigorous intermediate step of deriving equivalent discrete difference equations was not performed. For complete generality, Eqs. (66–68) with Eqs. (26), (30), and (55) should replace Eqs. (33–35), (26), (27), (30), and (31) for proper quantization error modeling as white noise.

## Setting Numerical Values for Quantization Noise Terms

In this section, we will address the problem of assigning numerical values to Eqs. (66–68) and (55) sensor quantization error terms for use in measurement and error state dynamic equation modeling. For either case, the quantization noise model will be based on the $\chi$-type sensor quantization noise parameter (see "Sensor Quantization Error Model" section) representing a zero mean uniformly distributed quantization error ranging from $-\varepsilon/2$ to $+\varepsilon/2$ in which $\varepsilon$ is the sensor pulse size. For such a random error characteristic, it is easily shown that the variance of

$\chi$ about its zero mean is $\varepsilon^2/12$. Equations (66–68) numerical noise models will be based on their equations (60–62) discrete version equivalents.

For the measurement modeling case, consider situations when an attitude- or velocity-type measurement is being made such that the measurement equation(s) include the attitude or velocity error parameters $\boldsymbol{\psi}^I$ and $\delta\boldsymbol{v}^I$. From Eq. (55), we see that, in terms of the revised error parameters $\boldsymbol{\psi}^{I*}$ and $\delta\boldsymbol{v}^{I*}$, the associated quantization error terms $\boldsymbol{\chi}_\alpha$ and $\boldsymbol{\chi}_\upsilon$ will appear as measurement noise in the measurement equation (with an associated $C_B^I$ coefficient). If we assume that each angular rate sensor has the same pulse size and similarly for the accelerometers, the covariances of the associated quantization measurement noise matrices are

$$V_{M_\alpha} = \mathcal{E}\Big[\big(C_B^I\boldsymbol{\chi}_\alpha\big)\big(C_B^I\boldsymbol{\chi}_\alpha\big)^T\Big] = C_B^I\mathcal{E}\big(\boldsymbol{\chi}_\alpha\boldsymbol{\chi}_\alpha^T\big)\big(C_B^I\big)^T$$

$$= C_B^I\big(u_{\alpha_{\text{quant}}}\text{I}\big)\big(C_B^I\big)^T = \big(\varepsilon_\alpha^2/12\big)\text{I}$$

$$V_{M_\upsilon} = \big(\varepsilon_\upsilon^2/12\big)\text{I} \tag{69}$$

For error state dynamic equation modeling using Eqs. (63) and (64) compared with Eq. (65), the white noise spectral density matrices associated with $\delta\boldsymbol{\alpha}_{\psi v_{\text{quant}}}$ and $\delta\boldsymbol{\alpha}_{\psi_{\text{quant}}}$ can be easily identified from the average rate of change of the $\boldsymbol{\psi}^{I*}$ and $\delta\boldsymbol{v}^{I*}$ covariances over an $m$ cycle. Recognizing from their definitions that $\delta\boldsymbol{\alpha}_{\psi v_{\text{quant}}}$ and $\delta\boldsymbol{\alpha}_{\psi_{\text{quant}}}$ are independent from one another with independent components, we find

$$Q_{\alpha\psi v} \approx \frac{\mathcal{E}\Big[\big(\Delta t_m\boldsymbol{\chi}_{\alpha\psi v_m}\big)\big(\Delta t_m\boldsymbol{\chi}_{\alpha\psi v_m}\big)^T\Big]}{\Delta t_m} = \mathcal{E}\Big[\boldsymbol{\chi}_{\alpha_{m-1}}\big(\boldsymbol{\chi}_{\alpha_{m-1}}\big)^T\Big]\Delta t_m$$

$$= \text{I}\frac{u_{\alpha_{\text{quant}}}}{f_m} = \text{I}\frac{\varepsilon_\alpha^2}{12f_m}$$

$$Q_{\alpha\psi} \approx \frac{\mathcal{E}\Big[\big(\Delta t_m\boldsymbol{\zeta}_{\alpha\psi_m}\big)\big(\Delta t_m\boldsymbol{\zeta}_{\alpha\psi_m}\big)^T\Big]}{\Delta t_m}$$

$$= \mathcal{E}\left[\left(\sum_{l=r(m-1)+2}^{l=rm}\boldsymbol{\chi}_{\alpha_{l-1}}\right)\left(\sum_{l=r(m-1)+2}^{l=rm}\boldsymbol{\chi}_{\alpha_{l-1}}\right)^T\right]\Delta t_m$$

$$= \text{I}\sum_{l=r(m-1)+2}^{l=rm}u_{\alpha_{\text{quant}}} = \text{I}(r-1)\frac{u_{\alpha_{\text{quant}}}}{f_m} = \text{I}\left(\frac{f_l}{f_m}-1\right)\frac{\varepsilon_\alpha^2}{12f_m} \tag{70}$$

Similar results apply for the $\upsilon$ accelerometer quantization error terms in Eqs. (67) and (68) when comparing with Eqs. (61) and (62). In summary with Eq. (69), we then find the following for the measurement and process noise terms.

White process noise spectral densities for propagation equations (66–68) are

$$Q_{\alpha\psi v} = \text{I}\big(\varepsilon_\alpha^2/12f_m\big), \qquad Q_{\alpha\psi} = \text{I}[f_l/f_m - 1]\big(\varepsilon_\alpha^2/12f_m\big) \tag{71}$$

$$Q_{\upsilon vR} = \text{I}\big(\varepsilon_\upsilon^2/12f_n\big), \qquad Q_{\upsilon v} = \text{I}[f_m/f_n - 1]\big(\varepsilon_\upsilon^2/12f_n\big) \tag{72}$$

Measurement noise covariances for Eqs. (55) are

$$V_{M_\alpha} = \big(\varepsilon_\alpha^2/12\big)\text{I}, \qquad V_{M_\upsilon} = \big(\varepsilon_\upsilon^2/12\big)\text{I} \tag{73}$$

## Application to Two-Speed Computation Algorithms

A fine point in the preceding discussion relates to values assigned to the $f_l$, $f_m$, and $f_n$ frequency terms in Eqs. (66) and (67) and Eqs. (71) and (72). These frequencies represent the rate at which attitude, velocity, and position parameters are updated in the strapdown system computer. However, what if two-speed algorithms [Refs. 4 (pp. 7-1–7-76), 5, 6, 10 (p. 354), and 11–17] are used for parameter updating? For example, let us say that angular rate sensor data are processed by a high-speed algorithm to calculate the change in attitude (in the form of a rotation vector) over a lower speed attitude update interval, with the rotation vector then used to update attitude at the lower rate. Which rate should be used for $f_l$ in Eqs. (66) and (71), the high-speed rate to generate the rotation vector or the lower speed attitude update rate? The answer is that the rotation vector computation frequency should be used for $f_l$. The rationale is provided heuristically next. A rigorous analytical proof is given in the Appendix.

The analytical theory behind two-speed attitude updating algorithms is that by computing the rotation vector at high speed and using it to update attitude at a lower speed, the overall accuracy is equivalent to what would be obtained by updating attitude at the high-speed rate. The analysis in this paper was based on updating attitude at a single rate $f_l$. Equivalent accuracy would be obtained from a two-speed algorithm if the rotation vector was updated at $f_l$ and the rotation vector was then used to update attitude at a lower rate. Hence, if an intermediate rotation vector is being calculated to update the attitude solution, the rotation vector computation rate would be used for $f_l$. With a single-speed algorithm, the algorithm input is the integrated angular rate sensor output over the attitude update cycle period (as in the simplified attitude update algorithm of this paper). This is equivalent to approximating the rotation vector calculation for the two-speed algorithm as a simple angular rate sensor output integral. For this case, the attitude algorithm update rate would be used for $f_l$.

From a different perspective, attitude change can be analytically defined as the sum of two elements, integrated angular rate plus the effect of coning motion [Refs. 4 (p. 7-9), 5, 12, and 14–17]. For two-speed attitude updating algorithms, the rotation vector computation at high speed accounts for both of these effects, with the integrated angular rate portion being the dominant term. Based on this interpretation, the preceding paragraph can be restated that, if coning is included in the rotation vector calculation, the coning algorithm update rate would be used for $f_l$. If coning is not included, the lower speed attitude update rate would be used for $f_l$.

Similar reasoning applies for the $f_m$ and $f_n$ values used for velocity/position updating. If sculling (in the acceleration transformation portion of velocity updating [Refs. 4 (p. 7–41), 6, 14, and 17]) or scrolling (for high resolution position updating [Refs. 4 (p. 7-62) and 6]) terms are being calculated at a higher rate than the basic velocity/position update frequencies, the sculling update rate would be used for $f_m$ and the scrolling rate for $f_n$. Otherwise $f_m$ and $f_n$ would be set to the velocity/position update frequencies.

## Numerical Examples

To illustrate the magnitude of system error effects generated by sensor quantization noise let us analyze a hypothetical situation in which the angular rate sensor pulse size $\varepsilon_\alpha$ is 1 arc-s with attitude and velocity updated at 1 kHz ($f_l$ and $f_m$). When Eqs. (71) are used, $Q_{\alpha\psi}$ is zero and the amplitude of $Q_{\alpha\psi v}$ is $\varepsilon_\alpha^2/(12f_m) = 8.33E{-}5$ arc-s$^2 s = 1.96E{-}15$ rad$^2$s. Consider how this white noise spectral density for $\delta\boldsymbol{\alpha}_{\psi v_{\text{quant}}}$ affects the $\boldsymbol{\psi}^{I*}$ attitude error in Eq. (66). Under a 1-rad/s angular rate [$\boldsymbol{\omega}^B$ in Eq. (66)], the amplitude of the white noise spectral density driving the $\boldsymbol{\psi}^{I*}$ covariance would be $(f_m/f_l)^2|\boldsymbol{\omega}^B|^2 Q_{\alpha\psi v_{\text{amplitude}}} = 1^2 \times 1^2 \times 1.96E{-}15$ rad$^2$/s $= 2.31E{-}8$ deg$^2$/h. The equivalent random walk on attitude coefficient is the square root or $1.52E{-}4$ deg/rt-h. For comparison, the random walk (on attitude) coefficient for a ring laser gyro (RLG) in a moderate accuracy aircraft inertial navigation system (INS) is $2E{-}3$ deg/rt-h. Thus, for the numerical example, the quantization noise effect is comfortably less (by a factor of 13) than the RLG random walk. Note also from Eq. (66) that under zero angular rate $\boldsymbol{\omega}^B$ the effect of quantization error on $\boldsymbol{\psi}^{I*}$ attitude error is zero.

Now consider that the analyst fails to recognize that angular rate sensor quantization error should be modeled as the derivative of white noise [i.e., Eqs. (4) with (6)] and instead, models $\delta\boldsymbol{\omega}_{\text{quant}}$ in Eq. (4) as white noise [i.e., uses $\delta\boldsymbol{\omega}_{\text{quant}}$ as white noise in Eq. (18) in place of $\delta\dot{\boldsymbol{\alpha}}_{\text{quant}}$]. This is equivalent to treating $\delta\alpha_{\text{quant}_l}$ in Eq. (2) as having two quantization errors ($\chi_{\alpha_l}$ and $\chi_{\alpha_{l-1}}$) with each $\delta\alpha_{\text{quant}_l}$ being independent from $l$ cycle to cycle. The corresponding random walk on attitude white noise spectral density would be $2f_l\varepsilon_\alpha^2/12$. (Note that the effect increases with update frequency in contrast with inverse frequency sensitivity for the correct $Q_{\alpha\psi v}$ modeling

earlier.) With the hypothesized 1-arc-s pulse size and 1-kHz attitude update rate, the mismodeling equates to $1.67E2$ arc-s$^2$/s = $3.92E{-}9$ rad$^2$/s = $4.63E{-}2$ deg$^2$/h. The corresponding random walk on attitude coefficient is the square root or $2.15E{-}1$ deg/rt-h. The effect is 108 time larger than the hypothesized $2E{-}3$ RLG random walk coefficient, clearly a serious mismodeling situation. Furthermore, from Eq. (18) (with $\delta\boldsymbol{\omega}_{\text{quant}}$ as white noise replacing $\delta\dot{\boldsymbol{\alpha}}_{\text{quant}}$), the random walk buildup on attitude error $\boldsymbol{\psi}^I$ is direct and independent of angular rate $\boldsymbol{\omega}^B$.

Consider the effect of $Q_{\alpha\psi v}$ (the white noise spectral density of $\delta\boldsymbol{\alpha}_{\psi v_{\text{quant}}}$) on velocity error equation (67) under zero angular rate conditions. Under zero angular rate, Eq. (66) shows zero coupling of $\delta\boldsymbol{\alpha}_{\psi v_{\text{quant}}}$ into $\dot{\boldsymbol{\psi}}^{I_*}$, hence, zero coupling of $\delta\boldsymbol{\alpha}_{\psi v_{\text{quant}}}$ into $\delta\boldsymbol{v}^{I_*}$ in Eq. (67) (through the $\boldsymbol{\psi}^{I_*}$ term). Quantization does impact $\delta\boldsymbol{v}^{I_*}$ in Eq. (67) through $\boldsymbol{a}^B_{\text{sf}}$ coupling. Under a 1-$g$ specific force acceleration $\boldsymbol{a}^B_{\text{sf}}$, the amplitude of the white noise spectral density driving the $\delta\boldsymbol{v}^{I_*}$ covariance would be $|\boldsymbol{a}^B_{\text{sf}}|^2 Q_{\alpha\psi v_{\text{amplitude}}} = (32.2\ \text{fps})^2 \times 1.96E{-}15\ \text{rad}^2/\text{s} = 2.03E{-}12\ (\text{fps})^2/\text{s}$. The equivalent random walk on velocity coefficient is the square root or $1.43E{-}6$ fps/rt-s = $8.55E{-}5$ fps/rt-h, negligible compared to the total velocity error in a moderate performance aircraft INS, which is on the order of 2 fps for the first hour of operation.

Again, consider that the analyst erroneously mismodels quantization error as white noise, that is, uses $\delta\boldsymbol{\omega}_{\text{quant}}$ as white noise in Eq. (18) in place of $\delta\dot{\boldsymbol{\alpha}}_{\text{quant}}$. The resulting attitude error $\boldsymbol{\psi}^I$ propagates through $\boldsymbol{a}^B_{\text{sf}}$ into velocity error equation (19). Reference 4, p. 13-104, shows that under the hypothesized 1-$g$ specific force environment, the velocity error variance response to random walk on attitude is $\frac{1}{3}g^2t^3q_{\omega\,\text{rand}}$, where $q_{\omega\,\text{rand}}$ is the random walk on attitude white noise spectral density, $g$ is gravity magnitude, and $t$ is time in navigation. For quantization error erroneously modeled as $q_{\omega\,\text{rand}}$ with the value given earlier (i.e., $3.92E{-}9$ rad$^2$/s) the resulting velocity variance increase at one hour would be $\frac{1}{3} \times 32.2^2 \times 3600^3 \times 3.93E{-}9 = 6.34\,E4\ (\text{fps})^2$ or 252 fps on a root-mean-square basis. This is $2.94\,E6$ times larger than the correct quantization noise effect and 126 times larger than the 2-fps moderate accurate INS total velocity error.

As a final example under approximately zero angular velocity conditions, let us hypothesize a quasi-stationary INS initial alignment situation where a Kalman filter is being used to estimate system initial heading using the horizontal components of $\boldsymbol{R}$ [Eqs. (7–9)] as the measurement. (The initial alignment process is discussed in detail in Ref. 4, pp. 6-1–6-9 and 14-36–14-80.) Reference 4, pp. 14-10–14-16 and 14-72–14-73, shows that angular rate sensor random walk on attitude error produces an estimated heading error at initial alignment completion given by $\sqrt{(q_{\omega\,\text{rand}}/T_{\text{align}})}/(\omega_e \cos\text{lat})$, where $q_{\omega\,\text{rand}}$ is the angular rate sensor random walk on attitude white noise spectral density [the spectral density for each element of $\delta\boldsymbol{\omega}_{\text{rand}}$ in Eq. (4)], $T_{\text{align}}$ is the time in alignment, $\omega_e$ is Earth rotation rate, and lat is latitude. The same reference also shows that angular rate sensor quantization error produces an error in estimated heading given by $\sqrt{(3q_{\alpha\,\text{quant}}/T^3_{\text{align}})}/(\omega_e \cos\text{lat})$, where $q_{\alpha\,\text{quant}}$ is the amplitude of the $Q_{\alpha\psi v}$ quantization white noise spectral density function in Eq. (71). Consider the case when lat = 45° and $T_{\text{align}} = 180$ s. When the earlier hypothesized RLG value for $q_{\omega\,\text{rand}}$ [$(2E{-}3)^2$ deg$^2$/h = $3.38E{-}13$ rad$^2$/s] is used, the earlier formula yields $8.43E{-}4$ rad contribution to heading error. (Note that the allowance for initial heading error in a moderate accuracy INS is typically on the order of $1E{-}3$ rad.) When the earlier computed $Q_{\alpha\psi v}$ amplitude for $q_{\alpha\,\text{quant}}$ ($1.96E{-}15$ rad$^2$ s) is used, the heading error formula gives $6.17E{-}7$ rad heading error due to angular rate sensor quantization. Thus, for the hypothesized pulse size, update frequencies, and alignment time, the initial heading error caused by angular rate sensor quantization error is negligible compared to that caused by random walk on attitude ($q_{\omega\,\text{rand}}$). Note also that if quantization error was incorrectly modeled as $q_{\omega\,\text{rand}}$ white noise at $3.92E{-}9$ rad$^2$/s (as discussed earlier), the $q_{\omega\,\text{rand}}$ into heading error formula would predict the estimated heading error to be $9.08E{-}2$ rad, significantly outside moderate accuracy INS accuracy specifications.

Similar methods can be used to analyze the effect of accelerometer quantization error and associated mismodeling on initial alignment accuracy. For heading error analysis, Ref. 4, pp. 14-10–14-16 and 14-72–14-73, shows that heading error caused by accelerometer quantization during initial alignment is $\sqrt{[20q_{v\,\text{quant}}/(g^2T^5_{\text{align}})]}/(\omega_e \cos\text{lat})$ where $g$ is gravity magnitude and $q_{v\,\text{quant}}$ is the amplitude of the $Q_{vvR}$ quantization white noise spectral density function in Eq. (72) [i.e., $\varepsilon_v^2/(12f_n)$]. The same reference also shows that accelerometer random walk on velocity error produces an estimated heading error of $\sqrt{[3q_{a\,\text{rand}}/(g^2T^3_{\text{align}})]}/(\omega_e \cos\text{lat})$ where $q_{a\,\text{rand}}$ is the accelerometer random walk on velocity white noise spectral density [the spectral density for each element of $\delta\boldsymbol{a}_{\text{rand}}$ in Eq. (5)].

## Validity Limits for Quantization Error as Random Noise

A fundamental assumption in the characterization of quantization error as random noise is statistical independence of the error from computation cycle to cycle. Under most navigation flight conditions, this is a reasonable assumption; however, there are those situations when the assumption is flawed. For example, consider the case where the angular rate is constant and low enough that only a single pulse is emitted from the associated angular rate sensor over several attitude/velocity update cycles (e.g., during quasi-stationary initial alignment when one of the angular rate sensor input axes is close to east with no external disturbances). Under these conditions, angular rate sensor quantization error produces an angular error between pulses that builds up linearly with time and is reset when each pulse is emitted [i.e., a sawtooth pattern with the ramping portion slope equal to the negative of the sensor input (as in Fig. 4)]. (A similar effect would also occur for an accelerometer when its input axis was near level.) The pattern repeats between pulses, and hence, is not random from computer cycle to cycle. From the nature of the repeating quantization sawtooth error pattern, resulting velocity/position errors would also be cyclic and have no amplitude buildup with time as with random-type error effects. Therefore, representation of quantization error as random is invalid. Note, however, that in terms of error buildup with time, approximating quantization error as random noise for this case is a conservative estimate of the actual effect (i.e., the actual effect is bounded). On the other hand, a cyclic sawtooth-type quantization error (if it exists) must still be analyzed independently to assess its particular effect on system performance.

For the static initial alignment scenario discussed, it is known that when the frequency of pulses (and the sawtooth error pattern) generated by angular rate sensor or accelerometer pulse quantization becomes low enough, the Kalman filter estimated heading develops noticeable transient error oscillations that can be large and lengthy enough to prohibit satisfactory convergence in the allocated alignment time. The expected performance effect can be predicted using Eqs. (33–35) for error propagation between Kalman updates, with the quantization error terms in question treated as cyclic sawtooth patterns. If the resulting heading error is unacceptable, it may be possible to reduce the quantization error using appropriate compensation techniques such as discussed next.

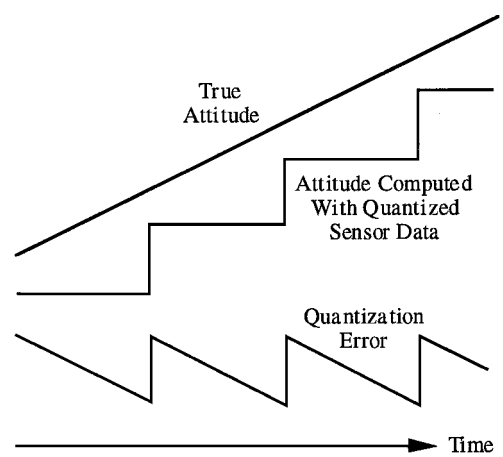


**Fig. 4 Attitude computed with quantized sensor data under constant angular rate.**

## Compensating for Sensor Pulse Quantization Error

Various methods have been used for reducing sensor pulse quantization error in inertial navigation systems. Fundamentally, if it is possible, the associated pulse size should be reduced. Alternatively, in some sensors, the integrated sensor input since the last pulse output (i.e., the pulse count "residual") can be measured electronically and used to correct the pulse count (Ref. 4, pp. 8-29–8-31). For such an implementation, the effective pulse size is reduced to the error in measuring the residual (e.g., 5% of the uncompensated pulse). A variation on this approach is to approximate the residual as the uncompensated pulse size multiplied by the ratio of a high-frequency clock count since the last pulse divided by the clock count between the last and previous pulse (Ref. 4, p. 8-29). The effective pulse size is thereby reduced by the reciprocal of the clock count between pulses. The latter technique is implicitly based on constant sensor input between pulses and loses its effectiveness when the time between pulses becomes long and random variations in sensor inputs are present. Each of the preceding approaches requires additional electronic elements in the sensor assembly.

A direct approach for overcoming the effect of low-frequency pulse quantization error is to assure that the output pulse rate from the sensors remains reasonably high, even under low sensor input conditions. The result is that the random quantization error model assumption remains valid under all conditions. This can be accomplished by providing an artificial electrical bias input to the sensor (if the design permits) or a mechanical bias. For each method, the bias can be constant or oscillatory with randomness added if necessary to ensure pulse count to count randomness. Means must then be provided for subtracting the bias from the sensor output before it is used in the navigation computations. For an oscillating bias, the error in removal can be included as part of the quantization error model.[3] An interesting application of the mechanical method is provided in the case of mechanically dithered RLGs whereby each gyro block is angularly vibrated at high frequency relative to the sensor assembly to avoid lock-in [Refs. 3 and 10, (p. 331)]. The resulting gyro dither motion also imparts a backreaction torque into the sensor assembly, which sets up a linear vibration of the accelerometers. The net result is that all sensors experience oscillatory inputs that generate randomness in resulting pulse count samples.

## Conclusions

Inertial sensor quantization error generally is a minor contributor to attitude/velocity/position and initial heading determination inaccuracy in a strapdown INS. However, mismodeling of quantization error effects can result in erroneously large estimates of their impact on INS performance. Unlike other sensor error sources, the magnitude of the quantization effect on system accuracy depends on the inertial system attitude/velocity/position computation update frequencies. In general, for proper quantization modeling, the higher the frequency, the smaller is the effect of quantization error. Mismodeling can falsely lead to the opposite conclusion, that is, higher update frequencies increasing quantization error contributions. For two-speed updating algorithms, the high-speed computation rate for coning, sculling, and scrolling is the determining frequency for quantization error modeling. Under low-frequency sensor input conditions, the assumption of randomness in sensor pulse quantization modeling deteriorates, and particular application-dependent models (e.g., cyclic sawtooth patterns) must be used for proper error characterization. The resulting effect on navigation accuracy can be analyzed using the differential error propagation equations derived in the paper with appropriate deterministic models for the quantization error terms. Several compensation techniques are available for potentially reducing pulse quantization error if necessary to meet system accuracy requirements.

## Appendix: Two-Speed vs Single-Speed Attitude Algorithm Response to Sensor Error

This Appendix provides a rigorous proof that the response of a two-speed attitude updating algorithm to angular rate sensor error is the same as that for a single-speed updating algorithm operating at the same update rate as the high-speed portion of the two-speed algorithm. By extension, this Appendix also shows that, for a two-speed updating algorithm (using low and high updating frequencies), sensor error effects that are update frequency dependent (such as quantization error) will be a function of only the high-speed updating frequency.

For a two-speed attitude updating algorithm [Refs. 4 (pp. 7-5–7-15), 5, 11, 12, and 14], let us define the basic $C_B^I$ attitude update to be performed at a $j$ cycle rate with $B_j$ defined as the orientation of the $B$ frame at the $j$ cycle time. Attitude is computed at the $j$ rate as

$$C_{B_j}^I = C_{B_{j-1}}^I C_{B_j}^{B_{j-1}} \tag{A1}$$

The $C_{B_j}^{B_{j-1}}$ matrix is calculated using a simplified high-speed integration algorithm over the $j-1$ to $j$ cycle times. For this analysis, we will use the $l$ index to represent the high-speed algorithm updating rate between $j-1$ and $j$.

From an analytical standpoint, the form of the high-speed integration algorithm is arbitrary so long as it is analytically correct (i.e., the analytical approximation error is negligible compared to inaccuracy generated from angular rate sensor input errors). Because of its simplified derivative form over small angle rotations, the attitude parameter selected for the high-speed integration is usually a rotation vector, which is then converted to $C_{B_j}^{B_{j-1}}$ at the $j$ update time for use in Eq. (A1). For expediency in this analysis, we will assume that the high-speed algorithm integration parameter is a direction cosine matrix so that the integrated result at time $j$ is $C_{B_j}^{B_{j-1}}$ directly. From an error analysis standpoint, it should be clear that either approach provides the same error effect in the $C_{B_j}^{B_{j-1}}$ matrix. Based on this rationale then, we multiply Eq. (7) on the left by the constant $C_I^{B_{j-1}}$ to find for the derivative form of the high-speed update operation:

$$\dot{C}_B^{B_{j-1}} = C_B^{B_{j-1}}(\boldsymbol{\omega}^B\times) \tag{A2}$$

When an initial value of identity is used, integrating Eq. (A2) from the $j-1$ to $j$ cycle times using a high-speed integration algorithm provides $C_{B_j}^{B_{j-1}}$ for Eq. (A1).

We will now analyze the effect of angular rate sensor error on the described two-speed attitude updating process compared with the single-speed attitude updating concept described in the body of the paper. First, we address the rotation angle error $\boldsymbol{\phi}^{B_{j-1}}$ in $C_B^{B_{j-1}}$ caused by angular rate sensor error. Following the same procedure that led to Eq. (49), we begin as in Eqs. (13) and (14):

$$\hat{C}_B^{B_{j-1}} = [\mathrm{I} - (\boldsymbol{\phi}^{B_{j-1}}\times)]C_B^{B_{j-1}}, \qquad \delta C_B^{B_{j-1}} = -(\boldsymbol{\phi}^{B_{j-1}}\times)C_B^{B_{j-1}} \tag{A3}$$

As in Eq. (36), a high-speed $l$ cycle algorithm will be used to integrate Eq. (A2):

$$C_{B_l}^{B_{j-1}} = C_{B_{l-1}}^{B_{j-1}} C_{B_l}^{B_{l-1}} \tag{A4}$$

Then, as in Eq. (49), the $C_B^{B_{j-1}}$ error $\boldsymbol{\phi}^{B_{j-1}}$ propagates in Eq. (A4) from $l-1$ to $l$ as

$$\boldsymbol{\phi}_l^{B_{j-1}} = \boldsymbol{\phi}_{l-1}^{B_{j-1}} - C_{B_{l-1}}^{B_{j-1}}\delta\boldsymbol{\alpha}_l \tag{A5}$$

The cumulative effect of Eq. (A5) at cycle $j$ is

$$\boldsymbol{\phi}_j^{B_{j-1}} = \sum_{\substack{\text{all } l \text{ from} \\ j-1 \text{ to } j}} \left(\boldsymbol{\phi}_l^{B_{j-1}} - \boldsymbol{\phi}_{l-1}^{B_{j-1}}\right) = -\sum_{\substack{\text{all } l \text{ from} \\ j-1 \text{ to } j}} C_{l-1}^{B_{j-1}}\delta\boldsymbol{\alpha}_l \tag{A6}$$

Equation (A6) defines the error $\boldsymbol{\phi}_j^{B_{j-1}}$ in $\hat{C}_{B_j}^{B_{j-1}}$ caused by angular rate sensor error. Now let us look and see how it effects the error in $C_{B_j}^I$ through Eq. (A1). The error in $C_{B_j}^I$ is the differential of Eq. (A1), which with Eq. (A3) at cycle $j$ is

$$\begin{aligned}\delta C_{B_j}^I &= \delta C_{B_{j-1}}^I C_{B_j}^{B_{j-1}} + C_{B_{j-1}}^I \delta C_{B_j}^{B_{j-1}} \\ &= \delta C_{B_{j-1}}^I C_{B_j}^{B_{j-1}} - C_{B_{j-1}}^I \left(\boldsymbol{\phi}_j^{B_{j-1}}\times\right) C_{B_j}^{B_{j-1}}\end{aligned} \tag{A7}$$

Using Eq. (14) in Eq. (A7) finds the equivalent in terms of the $\psi_j^I$ error in $\hat{C}_{B_j}^I$:

$$-\left(\psi_j^I\times\right)C_{B_j}^I = -\left(\psi_{j-1}^I\times\right)C_{B_{j-1}}^I C_{B_j}^{B_{j-1}} - C_{B_{j-1}}^I\left(\phi_j^{B_{j-1}}\times\right)C_{B_j}^{B_{j-1}} = -\left(\psi_{j-1}^I\times\right)C_{B_j}^I - C_{B_{j-1}}^I\left(\phi_j^{B_{j-1}}\times\right)C_{B_j}^{B_{j-1}} \tag{A8}$$

Multiplying on the right by $C_I^{B_j}$ then obtains

$$\begin{aligned}\left(\psi_j^I\times\right) &= \left(\psi_{j-1}^I\times\right) + C_{B_{j-1}}^I\left(\phi_j^{B_{j-1}}\times\right)C_{B_j}^{B_{j-1}}C_I^{B_j}\\ &= \left(\psi_{j-1}^I\times\right) + C_{B_{j-1}}^I\left(\phi_j^{B_{j-1}}\times\right)C_I^{B_{j-1}}\\ &= \left(\psi_{j-1}^I\times\right) + \left[\left(C_{B_{j-1}}^I\phi_j^{B_{j-1}}\right)\times\right]\end{aligned} \tag{A9}$$

or

$$\psi_j^I = \psi_{j-1}^I + C_{B_{j-1}}^I\phi_j^{B_{j-1}} \tag{A10}$$

When Eq. (A6) is substituted for $\phi_j^{B_{j-1}}$,

$$\psi_j^I = \psi_{j-1}^I - C_{B_{j-1}}^I\sum_{\substack{\text{all } l \text{ from}\\ j-1 \text{ to } j}} C_{B_{l-1}}^{B_{j-1}}\delta\boldsymbol{\alpha}_l = \psi_{j-1}^I - \sum_{\substack{\text{all } l \text{ from}\\ j-1 \text{ to } j}} C_{B_{l-1}}^I\delta\boldsymbol{\alpha}_l \tag{A11}$$

The cumulative effect when $j$ equals some cycle time $k$ is

$$\psi_k^I = \sum_{\substack{\text{all } j \text{ to}\\ \text{cycle } k}}\left(\psi_j^I - \psi_{j-1}^I\right) = -\sum_{\substack{\text{all } j \text{ to}\\ \text{cycle } k}}\sum_{\substack{\text{all } l \text{ from}\\ j-1 \text{ to } j}} C_{B_{l-1}}^{B_{j-1}}\delta\boldsymbol{\alpha}_l = -\sum_{\substack{\text{all } l \text{ to}\\ \text{cycle } k}} C_{B_{l-1}}^I\delta\boldsymbol{\alpha}_l \tag{A12}$$

Now consider what the $\psi_k^I$ error in $\hat{C}_B^I$ would be for a single-speed integration algorithm operating at the high-speed $l$ cycle rate. The answer has already been derived as Eq. (49) for which we can write for the cumulative effect at cycle $k$:

$$\psi_k^I = \sum_{\substack{\text{all } l \text{ to}\\ \text{cycle } k}}\left(\psi_l^I - \psi_{l-1}^I\right) = -\sum_{\substack{\text{all } l \text{ to}\\ \text{cycle } k}} C_{B_{l-1}}^I\delta\boldsymbol{\alpha}_l \tag{A13}$$

Equations (A12) and (A13) are identical. Thus, we see that for the two-speed attitude algorithm, inaccuracy caused by sensor error is identical to that of a single-speed algorithm operating at the two-speed algorithm high-speed computation rate (i.e., the $l$ cycle rate). This finding can be extrapolated to analytical results in the main body of the paper derived from Eq. (49), for example, Eq. (66) with Eq. (71), which have frequency $f_l$ dependent quantization error terms. Hence, for the two-speed attitude algorithm, Eqs. (66) with Eq. (71) also apply with $f_l$ corresponding to the high-speed $l$ cycle update frequency, not the lower speed $j$ cycle update frequency.

## References


[1] Chatfield, A. B., *Fundamentals of High Accuracy Inertial Navigation*, AIAA, Reston, VA, 1997, pp. 227–229.

[2] Rogers, R. M., *Applied Mathematics In Integrated Navigation Systems*, AIAA, Reston, VA, 2000, pp. 99–101.

[3] Savage, P. G., "Strapdown Sensors," *Strapdown Inertial Systems—Theory and Applications*, Lecture Series 95, AGARD, 1978, Sec. 2.

[4] Savage, P. G., *Strapdown Analytics*, Strapdown Associates, Inc., Maple Plain, MN, 2000.

[5] Savage, P. G., "Strapdown Inertial Navigation System Integration Algorithm Design, Part 1: Attitude Algorithms," *Journal of Guidance, Control, and Dynamics*, Vol. 21, No. 1, 1998, pp. 19–28.

[6] Savage, P. G., "Strapdown Inertial Navigation System Integration Algorithm Design, Part 2: Velocity and Position Algorithms," *Journal of Guidance, Control, and Dynamics*, Vol. 21, No. 2, 1998, pp. 208–221.

[7] Britting, K. R., *Inertial Navigation System Analysis*, Wiley, New York, 1971.

[8] Gelb, A., *Applied Optimal Estimation*, MIT Press, Cambridge, MA, 1978, p. 52.

[9] Brown, G. B., and Hwang, P. Y. C., *Introduction to Random Signals and Applied Kalman Filtering*, 3rd ed., Wiley, New York, 1997, p. 192.

[10] Kayton, M., and Fried, W. R., *Avionics Navigation Systems*, 2nd ed., Wiley, New York, 1997.

[11] Savage, P. G., "A New Second-Order Solution for Strapped-Down Attitude Computation," *AIAA/Joint Automatic Control Conference Proceedings Guidance and Control Conference*, 1966.

[12] Bortz, J. E., "A New Mathematical Formulation for Strapdown Inertial Navigation," *IEEE Transactions on Aerospace and Electronic Systems*, Volume AES-7, No. 1, 1971, pp. 61–66.

[13] Miller, R., "New Strapdown Attitude Algorithm," *Journal of Guidance, Control, and Dynamics*, Vol. 6, No. 4, 1983, pp. 287–291.

[14] Savage, P. G., "Strapdown System Algorithms," *Advances in Strapdown Inertial Systems*, Lecture Series 133, AGARD, 1984, Sec. 3.

[15] Ignagni, M. B., "Optimal Strapdown Attitude Integration Algorithms," *Journal of Guidance, Control, and Dynamics*, Vol. 13, No. 2, 1990, pp. 363–369.

[16] Ignagni, M. B., "Efficient Class of Optimized Coning Compensation Algorithms," *Journal of Guidance, Control, and Dynamics*, Vol. 19, No. 2, 1996, pp. 424–429.

[17] Roscoe, K. M., "Equivalency Between Strapdown Inertial Navigation Coning and Sculling Integrals/Algorithms," *Journal of Guidance, Control, and Dynamics*, Vol. 24, No. 2, 2001, pp. 201–205.